Published in final edited form as:
Neuroimage. 2019 October 01; 199: 545–552. doi:10.1016/j.neuroimage.2019.05.042.

The influence of brain iron on myelin water imaging

Christoph Birkl[1,2], **Anna Maria Birkl-Toeglhofer**[3,4], **Verena Endmayr**[5], **Romana Hoftberger**[5], **Gregor Kasprian**[6], **Claudia Krebs**[7], **Johannes Haybaeck**[3,4,8], **Alexander Rauscher**[1,9,10]

[1]UBC MRI Research Centre, University of British Columbia, Vancouver, BC, Canada

[2]Department of Neurology, Medical University of Graz, Austria

[3]Department of Pathology, Neuropathology and Molecular Pathology, Medical University of Innsbruck, Austria

[4]Diagnostic and Research Institute of Pathology, Medical University of Graz, Austria

[5]Institute of Neurology, Medical University of Vienna, Austria

[6]Department of Biomedical Imaging and Image-Guided Therapy, Medical University of Vienna, Austria

[7]Department of Cellular & Physiological Sciences, University of British Columbia, Vancouver, BC, Canada

[8]Department of Pathology, Medical Faculty, Otto-von-Guerecke University Magdeburg, Germany

[9]Department of Physics & Astronomy, University of British Columbia, Vancouver, BC, Canada

[10]Department of Pediatrics (Division of Neurology), University of British Columbia, Vancouver, BC, Canada

Abstract

With myelin playing a vital role in normal brain integrity and function and thus in various neurological disorders, myelin sensitive magnetic resonance imaging (MRI) techniques are of great importance. In particular, multi-exponential T_2 relaxation was shown to be highly sensitive to myelin. The myelin water imaging (MWI) technique allows to separate the T_2 decay into short components, specific to myelin water, and long components reflecting the intra- and extracellular water. The myelin water fraction (MWF) is the ratio of the short components to all components. In the brain's white matter (WM), myelin and iron are closely linked via the presence of iron in the myelin generating oligodendrocytes. Iron is known to decrease T_2 relaxation times and may therefore mimic myelin. In this study, we investigated if variations in WM iron content can lead to apparent MWF changes. We performed MWI in post mortem human brain tissue prior and after chemical iron extraction. Histology for iron and myelin confirmed a decrease in iron content and no change in myelin content after iron extraction. In MRI, iron extraction lead to a decrease in MWF by 26% to 28% in WM. Thus, a change in MWF does not necessarily reflect a change in

Correspondence to: Christoph Birkl.

Corresponding Author Christoph Birkl, PhD, UBC MRI Research Centre, University of British Columbia, M10 - Purdy Pavilion, 2221 Wesbrook Mall, Vancouver, BC V6T 2B5, E-mail: christoph.birkl@ubc.ca, Tel: +1 604 827 5462, Fax: +1 604 827 3339.

Europe PMC Funders Author Manuscripts

myelin content. This observation has important implications for the interpretation of MWI findings in previously published studies and future research.

Keywords

Myelin Water Imaging; brain; iron; myelin; white matter; quantitative MRI

Europe PMC Funders Author Manuscripts

1 Introduction

Myelin plays a critical role in maintaining normal brain function as it protects axons from mechanical and chemical insults (Duncan et al., 2017; Nave and Trapp, 2008) and facilitates rapid signal transduction (Miron and Franklin, 2014; Zalc et al., 2008). Myelin is a bilayer membrane of lipids and proteins wrapped around axons, and is created by oligodendrocytes in the central nervous system. In humans, brain myelination starts in the late 2nd trimester of pregnancy (Jakovcevski et al., 2009) and lasts until early adulthood (Deoni et al., 2015; Fields, 2008; Kinney et al., 1988), followed by a decrease in myelin content with aging (Peters, 2002; Wiggins et al., 1988). Breakdown of the myelin sheath due to demyelinating diseases, such as multiple sclerosis (MS) (Lassmann et al., 2007), or decompaction of the myelin sheath, for example due to trauma (Donovan et al., 2014; Weber et al., 2018; Wright et al., 2016), leads to disturbed signal transduction and widespread neurological deficits. Moreover, recent research has provided evidence for myelin plasticity in the human brain (Makinodan et al., 2012; Monje, 2018). Thus, the ability to non-invasively assess myelin content is of great importance in neuroscience. Several magnetic resonance imaging (MRI) techniques, such as magnetization transfer (Chen et al., 2008; Schmierer et al., 2004a), ultrashort echo time imaging (Sheth et al., 2016; Wilhelm et al., 2012), and the analysis of the multi-exponential signal decay, called myelin water imaging (MWI) (Groeschel et al., 2016; MacKay et al., 1994; Oh et al., 2007; Prasloski et al., 2012b), were shown to be sensitive to myelin. In particular, the myelin water fraction (MWF) determined with MWI has demonstrated strong correlation with histology and electron microscopy (Chen et al., 2017; Laule et al., 2008; Webb et al., 2003). These post mortem validation studies have led to the paradigm that MWF can be regarded as imaging biomarker for myelin. MWI has been applied to MS (Faizy et al., 2016; Oh et al., 2007; Vavasour et al., 2017), mild traumatic brain injury (Wright et al., 2016), spinal cord injury (Kozlowski et al., 2008), aging (Faizy et al., 2018), and schizophrenia (Flynn et al., 2003), among others. The biophysical basis of MWI is the multi-exponential nature of the MR signal decay, which is composed of contributions from several tissue compartments, each with characteristic decay times. At 3 Tesla, the signal from water trapped between the lipid bilayers of the myelin sheath decays relatively quickly with T_2 decay times of 10 ms to 30 ms (Menon and Allen, 1991; Whittall and MacKay, 1989). Water in the intra- and extracellular compartment corresponds to decay times ranging from 40 ms to 100 ms and the signal from cerebrospinal fluid (CSF) has decay times in the order of seconds. Therefore, decomposing the multi-exponential MR signal decay into its individual components allows the mapping of the fast decaying MWF signal relative to the overall signal. The data required for this approach can be acquired with multi spin echo sequences, such as Carr-Purcell-Meiboom-Gill (CPMG) sequence or more rapidly with a Gradient Echo Spin Echo (GRASE) sequence (Prasloski et al., 2012b). Since MWI

interprets all water with short decay times as myelin water, any T_2 influencing substance present in the brain can potentially cause a bias in MWI. The most relevant of these interfering substances is iron, as it is relatively abundant with 45 mg per kg tissue in WM and up to 250 mg per kg tissue in deep gray matter (HALLGREN and SOURANDER, 1958; Krebs et al., 2014). In WM, iron is mainly present in oligodendrocytes and thus closely linked to myelin, both structurally and metabolically (Connor and Menzies, 1996; Stephenson et al., 2014; Todorich et al., 2009). When myelin and oligodendrocytes break down, iron is released into the extracellular space and eventually removed (Hametner et al., 2013). If water protons diffuse through the microscopic magnetic field inhomogeneities induced by iron, the T_2 relaxation time is shortened (Gossuin et al., 2004; Schenck and Zimmerman, 2004; Vymazal et al., 1996). Iron's ability to shorten T_2 and its close link to myelin raise the concern whether changes in brain iron content are able to mimic changes in myelin on MWF maps. To answer this question, we measured MWF in post mortem human brain tissue samples before and after chemical iron extraction with an iron chelating agent (Fukunaga et al., 2010; Oh et al., 2013; Schenck et al., 2006). We show that removal of tissue iron leads to a significant decrease in MWF by about 25-28%, while histological staining for myelin remains unchanged. The influence of iron on MWI can therefore not be ignored.

2 Methods

2.1 Brain tissue

The study was approved by the local ethics committee. Brain tissue fixed in 4% formalin of four human brains (2 females) with an age at death of 60, 70, 73, and 81 years and a post mortem interval between death and autopsy of 9 to 24 hours (mean = 17 hours) were included in this study. None of the cases had a history of neurological disorders or a neurological cause of death. From each brain, two coronal and approximately 1 cm thick brain slices were used for the experiment. Each brain slice was cut in half, resulting in two groups of four specimens each. In group 1, one half underwent iron extraction and the other half was immersed in formalin. In group 2, one half was immersed in the buffer solution without iron chelator and the other half in formalin. All samples underwent MR imaging prior to the iron extraction procedure.

2.2 Iron extraction

Iron was extracted from the brain tissue slices by reductive dissolution using 2 mM sodium dithionite and 1 mM iron chelator desferrioxamine dissolved in phosphate buffered saline (PBS) at pH 7 (Fukunaga et al., 2010; Oh et al., 2013; Schenck et al., 2006). Iron extraction was performed for 12 days and the buffer solution was replaced every other day. For the buffer-only treatment 2 mM sodium dithionite were dissolved in PBS at pH 7. Each brain slice was kept in a separate container for iron extraction, buffer-only treatment, or storage in formalin.

2.3 MRI Scanning and Image Analysis

For image acquisition brain slices were put in a plastic container filled with PBS and imaged on a 3 T MRI system (Philips Achieva, Best, the Netherlands) prior (day 0) and after 12 days

of iron extraction and buffer treatment, respectively. MWI was performed using both a GRASE and a CPMG sequence. Both sequences had 32 echoes with a first echo time (TE) of 10 ms, ΔTE of 10 ms, and a resolution of 1 x 1 x 4 mm. The repetition time (TR) was 1100 ms for the GRASE and 1000 ms for the CPMG sequence. We acquired both the GRASE and CPMG sequence because GRASE is currently the most widely used rapid approach and CPMG is the MRI gold standard for estimating the MWF. For quantitative analysis, the T_2 distributions were calculated using a regularized non-negative least squares algorithm with correction for stimulated echoes (Prasloski et al., 2012a) and a T_2 range of 10 ms to 2.0 seconds (Prasloski et al., 2012b; Whittall et al., 1997; Whittall and MacKay, 1989). The multi exponential T_2 decay is expressed as a T_2 distribution. The short geometric mean (sgm) T_2 component was defined as the area of the T_2 distribution within 10 and 20 ms, the intra- and extracellular water geometric mean (mgm) T_2 component as the area of the T_2 distribution within 20 ms and 2 s and the global geometric mean (ggm) T_2 as the area of the entire T_2 distribution. The upper T_2 cut-off of 20 ms for the short T_2 component was selected based on the T_2 distributions, as shown in Fig. 3. Since formalin fixation shortens relaxation times (Birkl et al., 2016; Laule et al., 2008), the cut-off was shorter than *in vivo* at 3 T. The MWF was defined as the ratio of the area of short T_2 components to the area of all T_2 components. Median and range of the MWF, ggm T_2, sgm T_2, mgm T_2, and intra- and extracellular water fraction (mfr) were assessed in WM ROI's manually drawn in all subjects. Three ROI's, to cover a large part of the WM, were drawn per tissue slice.

2.4 Histology

Following imaging, all brain slices were processed according to standard neuropathological procedures including dehydration and embedding in paraffin. Paraffin-embedded tissue blocks were cut as 10 μm thick sections. Sections were stained with haematoxylin and eosin (H&E) (general pathology), Luxol fast blue-periodic acid Schiff (LFB-PAS for myelin) and diaminobenzidine (DAB)-enhanced Turnbull blue (TBB) staining (TBB for ferrous (Fe^{2+}) and ferric (Fe^{3+}) non-heme iron) (Hametner et al., 2013). All stained slices were scanned and digitized with an Agfa Duoscan® photo scanner at 800 pixels per inch and constant brightness conditions.

3 Results

3.1 Histology for Iron and Myelin

Successful iron extraction was demonstrated by decreased staining for iron, while staining for myelin remained unchanged (Fig. 1). To test for possible chemical effects other than those caused by the iron chelator, control tissue samples were immersed in the buffer solution, without the iron chelating agent. No change in iron or myelin content was observed in these control samples (Fig. 2).

3.2 MR Image Contrast

The image contrast of the 1st echo at TE = 10 ms between gray and white matter was changed after iron extraction. Visually, a decrease in MWF can also be observed in the iron extracted tissue samples. Buffer treatment showed no visual effects on both image contrast

and MWF. This behavior was comparable in both GRASE based and CPMG based MWI (Fig. 3).

3.3 MR Signal Relaxation Characteristics

Chemical iron extraction changed the distribution of WM T_2 relaxation times (Fig. 4). After iron extraction, both the short relaxation times below 20 ms, which are considered to reflect myelin water, and the long relaxation times, which are thought to represent intra- and extracellular water, showed a decrease in their peak amplitude and a shift in their peak position. Neither the myelin water peak nor the intra- and extracellular water peak were shifted across this threshold by iron extraction. The buffer treatment had a prolonging effect on the T_2 relaxation times of intra- and extracellular water.

3.4 Myelin Water Fraction

Quantitative analysis in manually defined WM regions of interest (ROI) showed that iron extraction lead to an apparent reduction in MWF by 26% from 0.19 (range 0.12 – 0.23) to 0.14 (0.08 – 0.17) ($p = 0.003$) measured with GRASE and by 28% from 0.18 (0.13 – 0.22) to 0.13 (0.10 – 0.18) ($p < 0.001$) measured with CPMG (Fig. 5). Control tissue samples immersed in formalin or in the buffer solution exhibited no change in MWF. After iron extraction, the ggm T_2 increased by 24% from 42.2 ms (34.9 – 52.2 ms) to 52.3 (45.1 – 56.5 ms) ms ($p = 0.001$) and by 31% from 41.2 ms (31.8 – 51.4 ms) to 54.0 ms (47.8 – 65.5 ms) ($p = 0.001$) measured with GRASE and CPMG, respectively (Fig. 6). In the samples treated with the buffer solution, ggm T_2 increased by 18% from 41.3 ms (32.3 – 51.4 ms) to 48.6 ms (38.5 – 52.3 ms) ($p = 0.003$) measured with GRASE and by 12% from 40.1 ms (33.0 – 43.4 ms) to 44.9 ms (39.0 – 51.5 ms) ($p < 0.001$) measured with CPMG. Control tissue samples kept in formalin showed no change in T_2. A complete list of all quantitative parameters of the multi-exponential T_2 decay analysis after iron extraction, buffer-only, and formalin treatment is presented in Table 1.

4 Discussion

Iron and myelin are known to be major contributors to MR signal relaxation in brain tissue (Duyn and Schenck, 2017; Langkammer et al., 2012a; Stüber et al., 2014). In the present work, we investigated the influence of iron on MWI, by performing MWI in post mortem human brain tissue before and after chemical iron extraction. Histological staining for iron and myelin confirmed the expected decrease in iron content, while the myelin content was not altered by the iron extraction procedure. After iron extraction, a decrease in MWF and an increase in ggm T_2 was observed. After buffer treatment a slight increase in ggm T_2 and mgm T_2 was observed in absence of any change in iron histology. The buffer treatment might have caused a change of iron's magnetic properties without affecting the iron content. Future experiments will be needed to further investigate this behavior.

In general, formalin fixation reduces the overall T_2 relaxation times and shifts the entire T_2 spectrum to lower values compared to *in vivo* brain (Laule et al., 2008). Therefore, the myelin water cut-off was chosen according to the T_2 distribution observed in our samples. The cut-off of 20 ms to separate the short and the long T_2 component was kept the same for

both GRASE and CPMG and for all analysis. Neither the iron extraction procedure nor the buffer-only treatment changed the T_2 distribution in a way that would have caused the T_2 components to leak across the cut-off and thus bias the MWF. Note that both CPMG and GRASE based MWI were almost equally affected by iron extraction, even though GRASE has slightly stronger T_2* weighting due to the two gradient echoes per spin echo. In order to distinguish effects due to the buffer from effects due to the actual iron extraction, a buffer-only experiment was performed. The absence of MWF changes in buffer treated tissue shows that it is indeed the iron removal that reduces the MWF. This finding is further supported by histology which showed no change in iron or myelin content after buffer treatment.

Our observations are in line with previous literature which reported an increase in overall T_2 after chemical iron extraction using the identical iron removal procedure as employed in the present work (Schenck et al., 2006). Using a dual echo spin echo scan, Schenck et al. reported an increase in T_2 after iron extraction in brain regions with high iron content, such as deep gray matter but also in regions with lower iron content, such as WM (Schenck et al., 2006). However, the influence of iron extraction on the multi-exponential T_2 decay and therefore on myelin quantification have not been investigated heretofore. In our experiments, the decrease in MWF after iron extraction ranged between 25-28% in WM, demonstrating that a measured change in MWF does not necessarily reflect a change in myelin content. The sensitivity of MWI to variations in brain iron content has therefore far reaching consequences for applications in neuroscience and medicine.

The most profound implications are expected in conditions where both myelin and iron are known to be affected. In MS, histology has shown progressive reduction of both myelin and iron in the entire WM over the course of the disease (Bagnato et al., 2018; Hametner et al., 2013). A reduction in iron content is also observed in MS lesions (Wiggermann et al., 2017), except for active lesions, where iron may be present within macrophages. The procedure performed in the present study removed large amounts but not all iron, resulting in a comparable iron loss as observed in post mortem specimens of MS. In a recent patient study, MWF was found to be significantly reduced in the normal appearing white matter (NAWM) in subjects with MS over the course of five years (Vavasour et al., 2017). In light of the present results, such a reduction in measured MWF may also be in part due to reduction in iron content due to MS. In MS treatment trials, increases in MWF can no longer be unequivocally interpreted as remyelination without an independent investigation of possible changes in iron content.

While there is a biological link between myelin and iron via the oligodendrocytes, these two substances don’t necessarily fluctuate in tandem. For example, with normal aging, there is a reduction in myelin but an increase in iron content (HALLGREN and SOURANDER, 1958; Peters, 2002). In early brain development, on the other hand, both myelin and iron content increase, more rapidly in the first years of life, followed by a progressively slower rate until late adolescence and early adulthood (HALLGREN and SOURANDER, 1958). Thus, changes in MWF due to an increase in myelin during development may be amplified by the concomitant increase in iron, whereas a loss of myelin with aging may be masked by age related increases in iron content.

Non-heme iron is not the only T_2 shortening agent in the brain. Calcifications, hemorrhages or venous blood also shorten the T_2 relaxation times. At 3 T the T_2 of venous blood is 32 ms (Zhao et al., 2007) and lies below the cut-off of 40 ms used *in vivo*, whereas at 7 T the blood's T_2 shortens to 13 ms (Yacoub et al., 2001), which is also below the recommended cut-off of 25 ms at this field strength (Wiggermann et al., 2018). Therefore, venous blood may mimic myelin at both 3 T and 7 T. Since the venous blood volume in WM is about 1.7 ml/100 g WM tissue (2/3 of total WM blood volume) (Doucette et al., 2018; Leenders et al., 1990), T_2 shortening due to venous blood may be non-negligible.

The influence of iron on MWF measurements begs the question which alternative methods may be used for myelin quantification or if MWI itself can be corrected for the effects of iron. One possible avenue may be MR methods that directly detect myelin via ultra-short echo time imaging or the characterization of the NMR spectral properties, without having to rely on the interaction of water with myelin (Wilhelm et al., 2012). Another myelin sensitive MRI technique is magnetization transfer imaging (MTI) which was shown in post mortem studies to correlate well with staining for myelin (Schmierer et al., 2007, 2004b). However, MTR is also influenced by tissue water content (Vavasour et al., 2011). Beside water, Langkammer et al. showed a negative correlation of MTR with iron content in post mortem brain tissue, which suggests that iron plays a role in MTR (Langkammer et al., 2012b). Alternatively, one could try to correct MWI itself using an independent measurement of brain iron content. The magnetic susceptibility and R_2* relaxation were both shown to be sensitive to tissue iron content (Langkammer et al., 2012c, 2010). So far, iron quantification with quantitative susceptibility mapping (QSM) and R_2* mapping has been restricted to structures with low myelin content, such as deep gray matter and was validated using mass spectrometry or histology (Langkammer et al., 2010; Sun et al., 2014; Walsh and Wilman, 2011). In WM, both iron and myelin are strong contributors to magnetic susceptibility and R_2* (Duyn and Schenck, 2017). Therefore, a simple correction for iron content based on QSM or R_2* is not obvious. One potential approach to separate the contributions of iron and myelin is via the different temperature dependencies of their magnetic properties, as described by Curie's law (Birkl et al., 2015). The temperature coefficient of R_2* as a measure for iron content without the confounding contributions from myelin can be derived from R_2* measurements at various temperatures (Birkl et al., 2018). Of course, such approach is only feasible in post mortem MRI and not applicable in human *in vivo* studies. A potential approach to differentiate between iron and myelin in vivo is based on the combination of R_2* and QSM (Schweser et al., 2011). Schweser et al. proposed a technique called SEMI-TWInS to simultaneously extract the contribution of iron and myelin on T_2* weighted images. Elkady et al. used combined R_2* and QSM to longitudinally assess changes in iron and myelin content of deep gray matter structures in subjects with MS compared to healthy controls (Elkady et al., 2018). Alternatively, the orientation dependency of R_2* in WM can be used to separate the tissue orientation dependent effects of myelin and the orientation independent effects of iron (Kor et al., 2019). By doing so, an average of iron and myelin content across the whole WM can be calculated. Using this approach, it was shown that in siblings of MS patients iron content was increased and the myelin content was similar compared to controls (Kor et al., 2019). However, spatial information is lost with this approach, as only global WM averages for iron and myelin content can be estimated.

The observed decrease in MWF after iron extraction could in principle be caused by a change in water content (Vavasour et al., 2017). If a change in water content was the driving force behind the decrease in MWF, an increase in water content by approximately 22% would be needed to decrease the MWF by 26% (Vavasour et al., 2017). This would result in a loss of approximately 10 ml of iron extraction solution during the treatment of the sample. As no change in iron extraction or buffer solution volume was measured when replacing the solutions, a water content driven change in MWF and T_2 is highly unlikely.

As iron influences the signal from all the water, one might hypothesize that a part of the intra-/extra-cellular water compartment affected by the presence of iron within oligodendrocytes has short enough T_2 to be mistaken as myelin water. As a result the amount of myelin water appears to be larger, while at the same time the amount of intra-/extra-cellular water appears to be smaller, than it is in reality, resulting in apparent increase in MWF. This hypothesis is consistent with the high apparent MWF observed in the deep gray matter (see Figure 4 in (Prasloski et al., 2012b), for example), which is rich in iron but poor in myelin. Once the iron is removed from the oligodendrocytes, the short and long T_2 water compartments better represent myelin and intra-/extra-cellular water respectively, resulting in smaller, and more accurate MWF values.

In conclusion, our study shows that a measured change in MWF does not necessarily reflect an actual change in myelin content. Future research will have to take the effects of tissue iron into account and existing literature may require re-interpretation.

Acknowledgments

This study was funded by the Austrian Science Fund (FWF) project number J 4038 and by the National MS Society (RG 1507 05301). The authors thank Prof. Alex L MacKay and Prof. Piotr Kozlowski for useful comments and discussions.

References

Bagnato F, Hametner S, Boyd E, Endmayr V, Shi Y, Ikonomidou V, Chen G, Pawate S, Lassmann H, Smith S, Brian Welch E. Untangling the R2* contrast in multiple sclerosis: A combined MRI-histology study at 7.0 Tesla. PLoS One. 2018; 13:1–19. DOI: 10.1371/journal.pone.0193839

Birkl C, Carassiti D, Hussain F, Langkammer C, Enzinger C, Fazekas F, Schmierer K, Ropele S. Assessment of ferritin content in multiple sclerosis brains using temperature-induced R2* changes. Magn Reson Med. 2018; 79:1609–1615. DOI: 10.1002/mrm.26780 [PubMed: 28618066]

Birkl C, Langkammer C, Golob-Schwarzl N, Leoni M, Haybaeck J, Goessler W, Fazekas F, Ropele S. Effects of formalin fixation and temperature on MR relaxation times in the human brain. NMR Biomed. 2016; 29:458–465. DOI: 10.1002/nbm.3477 [PubMed: 26835664]

Birkl C, Langkammer C, Krenn H, Goessler W, Ernst C, Haybaeck J, Stollberger R, Fazekas F, Ropele S. Iron mapping using the temperature dependency of the magnetic susceptibility. Magn Reson Med. 2015; 73:1282–8. DOI: 10.1002/mrm.25236 [PubMed: 24752873]

Chen HS-M, Holmes N, Liu J, Tetzlaff W, Kozlowski P. Validating myelin water imaging with transmission electron microscopy in a rat spinal cord injury model. Neuroimage. 2017; 153:122–130. DOI: 10.1016/j.neuroimage.2017.03.065 [PubMed: 28377211]

Canadian MS/BMT Study Group. Chen JT, Collins DL, Atkins HL, Freedman MS, Arnold DL. Magnetization transfer ratio evolution with demyelination and remyelination in multiple sclerosis lesions. Ann Neurol. 2008; 63:254–62. DOI: 10.1002/ana.21302 [PubMed: 18257039]

Connor JR, Menzies SL. Relationship of iron to oligodendrocytes and myelination. Glia. 1996; 17:83–93. DOI: 10.1002/(SICI)1098-1136(199606)17:2<83::AID-GLIA1>3.0.CO;2-7 [PubMed: 8776576]

Deoni SCL, Dean DC, Remer J, Dirks H, O'Muircheartaigh J. Cortical maturation and myelination in healthy toddlers and young children. Neuroimage. 2015; 115:147–61. DOI: 10.1016/j.neuroimage.2015.04.058 [PubMed: 25944614]

Donovan V, Kim C, Anugerah AK, Coats JS, Oyoyo U, Pardo AC, Obenaus A. Repeated mild traumatic brain injury results in long-term white-matter disruption. J Cereb Blood Flow Metab. 2014; 34:715–23. DOI: 10.1038/jcbfm.2014.6 [PubMed: 24473478]

Doucette J, Wei L, Hernández-Torres E, Kames C, Forkert ND, Aamand R, Lund TE, Hansen B, Rauscher A. Rapid solution of the Bloch-Torrey equation in anisotropic tissue: Application to dynamic susceptibility contrast MRI of cerebral white matter. Neuroimage. 2018; 185:198–207. DOI: 10.1016/j.neuroimage.2018.10.035 [PubMed: 30332614]

Duncan ID, Marik RL, Broman AT, Heidari M. Thin myelin sheaths as the hallmark of remyelination persist over time and preserve axon function. Proc Natl Acad Sci U S A. 2017; 114:E9685–E9691. DOI: 10.1073/pnas.1714183114 [PubMed: 29078396]

Duyn JH, Schenck J. Contributions to magnetic susceptibility of brain tissue. NMR Biomed. 2017; 30 doi: 10.1002/nbm.3546

Elkady AM, Cobzas D, Sun H, Blevins G, Wilman AH. Discriminative analysis of regional evolution of iron and myelin/calcium in deep gray matter of multiple sclerosis and healthy subjects. J Magn Reson Imaging. 2018; doi: 10.1002/jmri.26004

Faizy TD, Kumar D, Broocks G, Thaler C, Flottmann F, Leischner H, Kutzner D, Hewera S, Dotzauer D, Stellmann J-P, Reddy R, et al. Age-Related Measurements of the Myelin Water Fraction derived from 3D multi-echo GRASE reflect Myelin Content of the Cerebral White Matter. Sci Rep. 2018; 8 14991 doi: 10.1038/s41598-018-33112-8 [PubMed: 30301904]

Faizy TD, Thaler C, Kumar D, Sedlacik J, Broocks G, Grosser M, Stellmann J-P, Heesen C, Fiehler J, Siemonsen S. Heterogeneity of Multiple Sclerosis Lesions in Multislice Myelin Water Imaging. PLoS One. 2016; 11:e0151496. doi: 10.1371/journal.pone.0151496 [PubMed: 26990645]

Fields RD. White matter in learning, cognition and psychiatric disorders. Trends Neurosci. 2008; 31:361–70. DOI: 10.1016/j.tins.2008.04.001 [PubMed: 18538868]

Flynn SW, Lang DJ, Mackay AL, Goghari V, Vavasour IM, Whittall KP, Smith GN, Arango V, Mann JJ, Dwork AJ, Falkai P, et al. Abnormalities of myelination in schizophrenia detected in vivo with MRI, and post-mortem with analysis of oligodendrocyte proteins. Mol Psychiatry. 2003; 8:811–20. DOI: 10.1038/sj.mp.4001337 [PubMed: 12931208]

Fukunaga M, Li T-Q, van Gelderen P, de Zwart Ja, Shmueli K, Yao B, Lee J, Maric D, Aronova Ma, Zhang G, Leapman RD, et al. Layer-specific variation of iron content in cerebral cortex as a source of MRI contrast. Proc Natl Acad Sci U S A. 2010; 107:3834–9. DOI: 10.1073/pnas.0911177107 [PubMed: 20133720]

Gossuin Y, Muller RN, Gillis P. Relaxation induced by ferritin: A better understanding for an improved MRI iron quantification. NMR Biomed. 2004; 17:427–432. DOI: 10.1002/nbm.903 [PubMed: 15526352]

Groeschel S, Hagberg GE, Schultz T, Balla DZ, Klose U, Hauser T-K, Nägele T, Bieri O, Prasloski T, MacKay AL, Krägeloh-Mann I, et al. Assessing White Matter Microstructure in Brain Regions with Different Myelin Architecture Using MRI. PLoS One. 2016; 11:e0167274. doi: 10.1371/journal.pone.0167274 [PubMed: 27898701]

Hallgren B, Sourander P. The effect of age on the non-haemin iron in the human brain. J Neurochem. 1958; 3:41–51. [PubMed: 13611557]

Hametner S, Wimmer I, Haider L, Pfeifenbring S, Brück W, Lassmann H, Pfeifenbring S, Br W. Iron and neurodegeneration in the multiple sclerosis brain. Ann Neurol. 2013; 74:848–861. DOI: 10.1002/ana.23974 [PubMed: 23868451]

Jakovcevski I, Filipovic R, Mo Z, Rakic S, Zecevic N. Oligodendrocyte development and the onset of myelination in the human fetal brain. Front Neuroanat. 2009; 3:5. doi: 10.3389/neuro.05.005.2009 [PubMed: 19521542]

Kinney HC, Brody BA, Kloman AS, Gilles FH. Sequence of central nervous system myelination in human infancy. II. Patterns of myelination in autopsied infants. J Neuropathol Exp Neurol. 1988; 47:217–34. [PubMed: 3367155]

Europe PMC Funders Author Manuscripts

Kor D, Birkl C, Ropele S, Doucette J, Xu T, Hernández-Torres E, Wiggermann V, Hametner S, Rauscher A. The role of iron and myelin in orientation dependent R2* of white matter. NMR Biomed. 2019; doi: 10.1002/nbm.4092

Kozlowski P, Raj D, Liu J, Lam C, Yung AC, Tetzlaff W. Characterizing white matter damage in rat spinal cord with quantitative MRI and histology. J Neurotrauma. 2008; 25:653–76. DOI: 10.1089/neu.2007.0462 [PubMed: 18578635]

Krebs N, Langkammer C, Goessler W, Ropele S, Fazekas F, Yen K, Scheurer E. Assessment of trace elements in human brain using inductively coupled plasma mass spectrometry. J Trace Elem Med Biol. 2014; 28:1–7. DOI: 10.1016/j.jtemb.2013.09.006 [PubMed: 24188895]

Langkammer C, Krebs N, Goessler W, Scheurer E, Ebner F, Yen K, Fazekas F, Ropele S. Quantitative MR Imaging of Brain Iron : A Postmortem Validation Study. Radiology. 2010; 257:455–462. DOI: 10.1148/radiol.10100495 [PubMed: 20843991]

Langkammer C, Krebs N, Goessler W, Scheurer E, Yen K, Fazekas F, Ropele S. Susceptibility induced gray-white matter MRI contrast in the human brain. Neuroimage. 2012a; 59:1413–9. DOI: 10.1016/j.neuroimage.2011.08.045 [PubMed: 21893208]

Langkammer C, Krebs N, Goessler W, Scheurer E, Yen K, Fazekas F, Ropele S. Susceptibility induced gray–white matter MRI contrast in the human brain. Neuroimage. 2012b; 59:1413–1419. DOI: 10.1016/j.neuroimage.2011.08.045 [PubMed: 21893208]

Langkammer C, Schweser F, Krebs N, Deistung A, Goessler W, Scheurer E, Sommer K, Reishofer G, Yen K, Fazekas F, Ropele S, et al. Quantitative susceptibility mapping (QSM) as a means to measure brain iron? A post mortem validation study. Neuroimage. 2012c; 62:1593–1599. DOI: 10.1016/j.neuroimage.2012.05.049 [PubMed: 22634862]

Lassmann H, Brück W, Lucchinetti CF. The immunopathology of multiple sclerosis: an overview. Brain Pathol. 2007; 17:210–8. DOI: 10.1111/j.1750-3639.2007.00064.x [PubMed: 17388952]

Laule C, Kozlowski P, Leung E, Li DKB, Mackay AL, Moore GRW. Myelin water imaging of multiple sclerosis at 7 T: correlations with histopathology. Neuroimage. 2008; 40:1575–80. DOI: 10.1016/j.neuroimage.2007.12.008 [PubMed: 18321730]

Leenders KL, Perani D, Lammertsma AA, Heather JD, Buckingham P, Healy MJ, Gibbs JM, Wise RJ, Hatazawa J, Herold S. Cerebral blood flow, blood volume and oxygen utilization. Normal values and effect of age. Brain. 1990; 113(Pt 1):27–47. [PubMed: 2302536]

MacKay A, Whittall K, Adler J, Li D, Paty D, Graeb D. In vivo visualization of myelin water in brain by magnetic resonance. Magn Reson Med. 1994; 31:673–7. [PubMed: 8057820]

Makinodan M, Rosen KM, Ito S, Corfas G. A critical period for social experience-dependent oligodendrocyte maturation and myelination. Science. 2012; 337:1357–60. DOI: 10.1126/science.1220845 [PubMed: 22984073]

Menon RS, Allen PS. Application of continuous relaxation time distributions to the fitting of data from model systems and excised tissue. Magn Reson Med. 1991; 20:214–27. [PubMed: 1775048]

Miron VE, Franklin RJM. Macrophages and CNS remyelination. J Neurochem. 2014; 130:165–71. DOI: 10.1111/jnc.12705 [PubMed: 24601941]

Monje M. Myelin Plasticity and Nervous System Function. Annu Rev Neurosci. 2018; 41:61–76. DOI: 10.1146/annurev-neuro-080317-061853 [PubMed: 29986163]

Nave K-A, Trapp BD. Axon-glial signaling and the glial support of axon function. Annu Rev Neurosci. 2008; 31:535–61. DOI: 10.1146/annurev.neuro.30.051606.094309 [PubMed: 18558866]

Oh J, Han ET, Lee MC, Nelson SJ, Pelletier D. Multislice brain myelin water fractions at 3T in multiple sclerosis. J Neuroimaging. 2007; 17:156–63. DOI: 10.1111/j.1552-6569.2007.00098.x [PubMed: 17441837]

Oh S-H, Kim Y-B, Cho Z-H, Lee J. Origin of B0 orientation dependent R2(*) (=1/T2(*)) in white matter. Neuroimage. 2013; 73:71–9. DOI: 10.1016/j.neuroimage.2013.01.051 [PubMed: 23376494]

Peters A. The effects of normal aging on myelin and nerve fibers: a review. J Neurocytol. 2002; 31:581–93. DOI: 10.1023/A:1025731309829 [PubMed: 14501200]

Prasloski T, Mädler B, Xiang Q-S, MacKay A, Jones C. Applications of stimulated echo correction to multicomponent T2 analysis. Magn Reson Med. 2012a; 67:1803–14. DOI: 10.1002/mrm.23157 [PubMed: 22012743]

Prasloski T, Rauscher A, MacKay AL, Hodgson M, Vavasour IM, Laule C, Mädler B. Rapid whole cerebrum myelin water imaging using a 3D GRASE sequence. Neuroimage. 2012b; 63:533–539. DOI: 10.1016/j.neuroimage.2012.06.064 [PubMed: 22776448]

Schenck JF, Zimmerman Ea. High-field magnetic resonance imaging of brain iron: birth of a biomarker? NMR Biomed. 2004; 17:433–45. DOI: 10.1002/nbm.922 [PubMed: 15523705]

Schenck JF, Zimmerman EA, Li Z, Adak S, Saha A, Tandon R, Fish KM, Belden C, Gillen RW, Barba A, Henderson DL, et al. High-field magnetic resonance imaging of brain iron in Alzheimer disease. Top Magn Reson Imaging. 2006; 17:41–50. DOI: 10.1097/01.rmr.0000245455.59912.40 [PubMed: 17179896]

Schmierer K, Scaravilli F, Altmann DR, Barker GJ, Miller DH. Magnetization transfer ratio and myelin in postmortem multiple sclerosis brain. Ann Neurol. 2004a; 56:407–15. DOI: 10.1002/ana.20202 [PubMed: 15349868]

Schmierer K, Scaravilli F, Altmann DR, Barker GJ, Miller DH. Magnetization transfer ratio and myelin in postmortem multiple sclerosis brain. Ann Neurol. 2004b; 56:407–415. DOI: 10.1002/ana.20202 [PubMed: 15349868]

Schmierer K, Tozer DJ, Scaravilli F, Altmann DR, Barker GJ, Tofts PS, Miller DH. Quantitative magnetization transfer imaging in postmortem multiple sclerosis brain. J Magn Reson Imaging. 2007; 26:41–51. DOI: 10.1002/jmri.20984 [PubMed: 17659567]

Schweser F, Deistung A, Lehr BW, Sommer K, Reichenbach JR. SEMI-TWInS : Simultaneous Extraction of Myelin and Iron using a T 2 * -Weighted Imaging Sequence. Proc Intl Soc Mag Reson Med. 2011; 19:120.

Sheth V, Shao H, Chen J, Vandenberg S, Corey-Bloom J, Bydder GM, Du J. Magnetic resonance imaging of myelin using ultrashort Echo time (UTE) pulse sequences: Phantom, specimen, volunteer and multiple sclerosis patient studies. Neuroimage. 2016; 136:37–44. DOI: 10.1016/j.neuroimage.2016.05.012 [PubMed: 27155128]

Stephenson E, Nathoo N, Mahjoub Y, Dunn JF, Yong VW. Iron in multiple sclerosis: roles in neurodegeneration and repair. Nat Rev Neurol. 2014; 10:459–68. DOI: 10.1038/nrneurol.2014.118 [PubMed: 25002107]

Stüber C, Morawski M, Schäfer A, Labadie C, Wähnert M, Leuze C, Streicher M, Barapatre N, Reimann K, Geyer S, Spemann D, et al. Myelin and iron concentration in the human brain: A quantitative study of MRI contrast. Neuroimage. 2014; 93(Pt 1):95–106. DOI: 10.1016/j.neuroimage.2014.02.026 [PubMed: 24607447]

Sun H, Walsh AJ, Lebel RM, Blevins G, Catz I, Lu J-Q, Johnson ES, Emery DJ, Warren KG, Wilman AH. Validation of quantitative susceptibility mapping with Perls' iron staining for subcortical gray matter. Neuroimage. 2014; doi: 10.1016/j.neuroimage.2014.11.010

Todorich B, Pasquini JM, Garcia CI, Paez PM, Connor JR. Oligodendrocytes and myelination: the role of iron. Glia. 2009; 57:467–78. DOI: 10.1002/glia.20784 [PubMed: 18837051]

Vavasour IM, Huijskens SC, Li DKB, Traboulsee AL, Mädler B, Kolind SH, Rauscher A, Moore GWRW, MacKay AL, Laule C. Global loss of myelin water over 5 years in multiple sclerosis normal-appearing white matter. Mult Scler. 2017; 24:1–12.

Vavasour IM, Laule C, Li DKB, Traboulsee AL, Mackay AL. Is the Magnetization Transfer Ratio a Marker for Myelin in Multiple Sclerosis? 2011; 718:713–718. DOI: 10.1002/jmri.22441

Vymazal J, Brooks RA, Baumgarner C, Tran V, Katz D, Bulte JW, Bauminger R, Di Chiro G. The relation between brain iron and NMR relaxation times: an in vitro study. Magn Reson Med. 1996; 35:56–61. [PubMed: 8771022]

Walsh AJ, Wilman AH. Susceptibility phase imaging with comparison to R2 mapping of iron-rich deep grey matter. Neuroimage. 2011; 57:452–61. DOI: 10.1016/j.neuroimage.2011.04.017 [PubMed: 21513807]

Webb S, Munro CA, Midha R, Stanisz GJ. Is multicomponent T2 a good measure of myelin content in peripheral nerve? Magn Reson Med. 2003; 49:638–45. DOI: 10.1002/mrm.10411 [PubMed: 12652534]

Weber AM, Pukropski A, Kames C, Jarrett M, Dadachanji S, Taunton J, Li DKB, Rauscher A. Pathological Insights From Quantitative Susceptibility Mapping and Diffusion Tensor Imaging in

Ice Hockey Players Pre and Post-concussion. Front Neurol. 2018; 9:575. doi: 10.3389/fneur.2018.00575 [PubMed: 30131752]

Whittall KP, MacKay AL. Quantitative interpretation of NMR relaxation data. J Magn Reson. 1989; 84:134–152. DOI: 10.1016/0022-2364(89)90011-5

Whittall KP, MacKay AL, Graeb DA, Nugent RA, Li DK, Paty DW. In vivo measurement of T2 distributions and water contents in normal human brain. Magn Reson Med. 1997; 37:34–43. [PubMed: 8978630]

Wiggermann V, Hametner S, Hernández-Torres E, Kames C, Endmayr V, Kasprian G, Höftberger R, Li DKB, Traboulsee A, Rauscher A. Susceptibility-sensitive MRI of multiple sclerosis lesions and the impact of normal-appearing white matter changes. NMR Biomed. 2017; 30:e3727. doi: 10.1002/nbm.3727

Wiggermann V, MacKay AL, Helms G, Rauscher A. In vivo high field myelin water imaging: Investigating the T2 distribution at 7T. Proc Intl Soc Mag Reson Med (Paris). 2018

Wiggins RC, Gorman A, Rolsten C, Samorajski T, Ballinger WE, Freund G. Effects of aging and alcohol on the biochemical composition of histologically normal human brain. Metab Brain Dis. 1988; 3:67–80. [PubMed: 3211076]

Wilhelm MJ, Ong HH, Wehrli SL, Li C, Tsai P-H, Hackney DB, Wehrli FW. Direct magnetic resonance detection of myelin and prospects for quantitative imaging of myelin density. Proc Natl Acad Sci U S A. 2012; 109:9605–10. DOI: 10.1073/pnas.1115107109 [PubMed: 22628562]

Wright AD, Jarrett M, Vavasour I, Shahinfard E, Kolind S, van Donkelaar P, Taunton J, Li D, Rauscher A. Myelin Water Fraction Is Transiently Reduced after a Single Mild Traumatic Brain Injury--A Prospective Cohort Study in Collegiate Hockey Players. PLoS One. 2016; 11:e0150215. doi: 10.1371/journal.pone.0150215 [PubMed: 26913900]

Yacoub E, Shmuel A, Pfeuffer J, Van De Moortele PF, Adriany G, Andersen P, Vaughan JT, Merkle H, Ugurbil K, Hu X. Imaging brain function in humans at 7 Tesla. Magn Reson Med. 2001; 45:588–94. [PubMed: 11283986]

Zalc B, Goujet D, Colman D. The origin of the myelination program in vertebrates. Curr Biol. 2008; 18:R511–2. DOI: 10.1016/j.cub.2008.04.010 [PubMed: 18579089]

Zhao JM, Clingman CS, Närväinen MJ, Kauppinen RA, van Zijl PCM. Oxygenation and hematocrit dependence of transverse relaxation rates of blood at 3T. Magn Reson Med. 2007; 58:592–7. DOI: 10.1002/mrm.21342 [PubMed: 17763354]

Europe PMC Funders Author Manuscripts

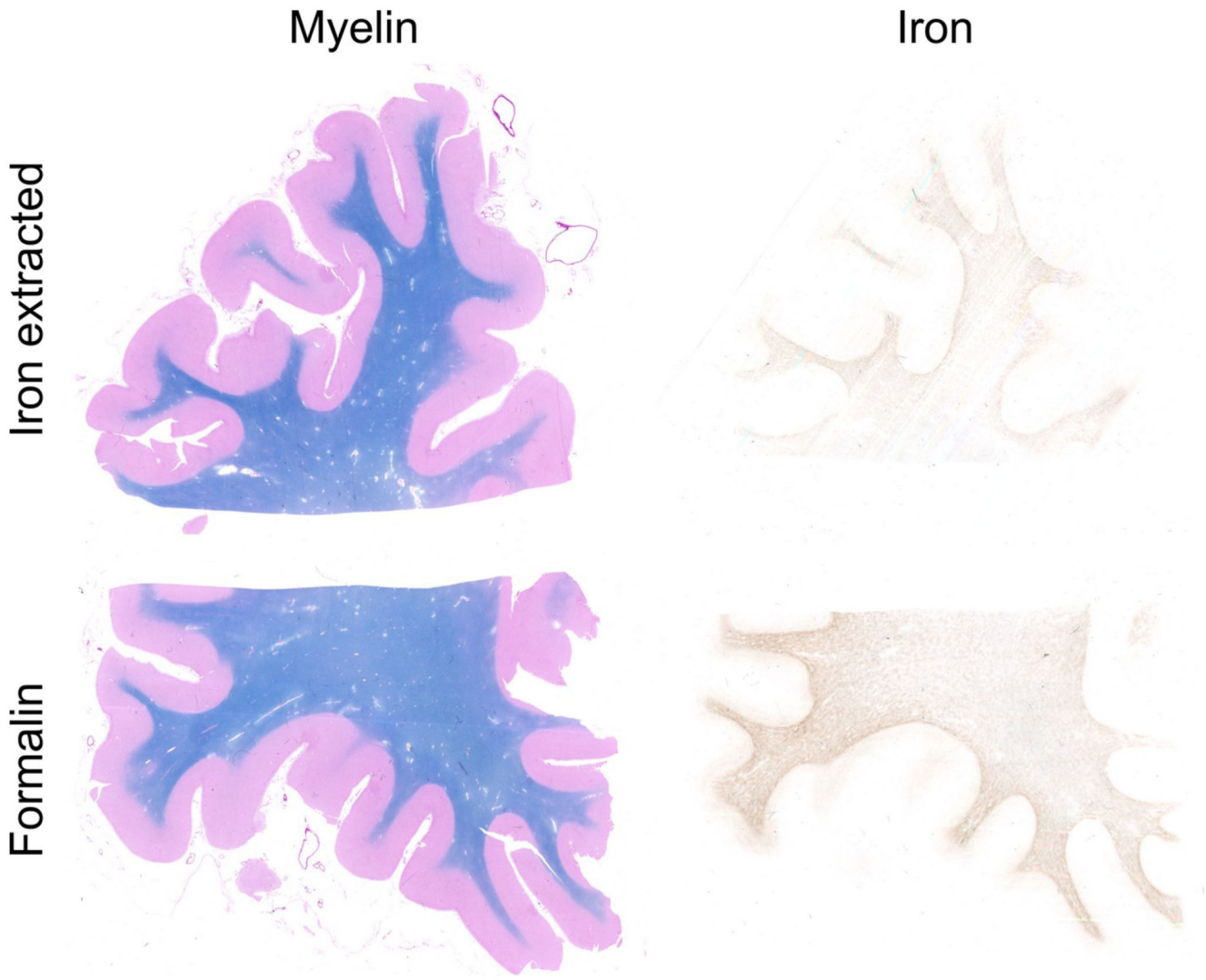

Fig. 1.
Staining for myelin (left) and iron (right) of a brain slice after chemical iron extraction (top) and a brain slice stored in formalin as reference (bottom). Myelin is not affected, whereas iron content is decreased.

Europe PMC Funders Author Manuscripts

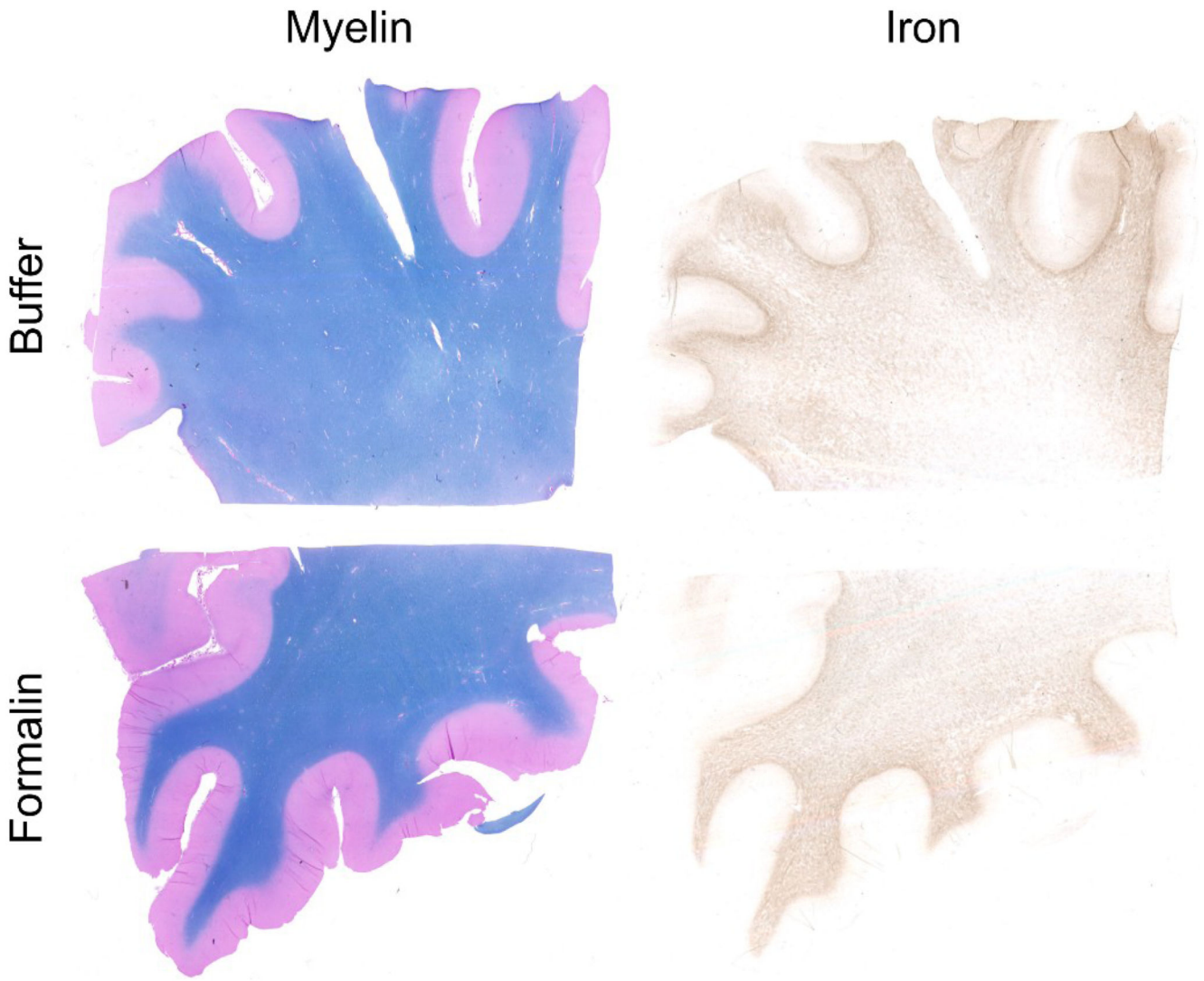

Fig. 2.

Staining for myelin (left) and iron (right) of a brain slice treated with the buffer solution without iron chelator (top) and a brain slice stored in formalin (bottom). Both, myelin and iron show no difference.

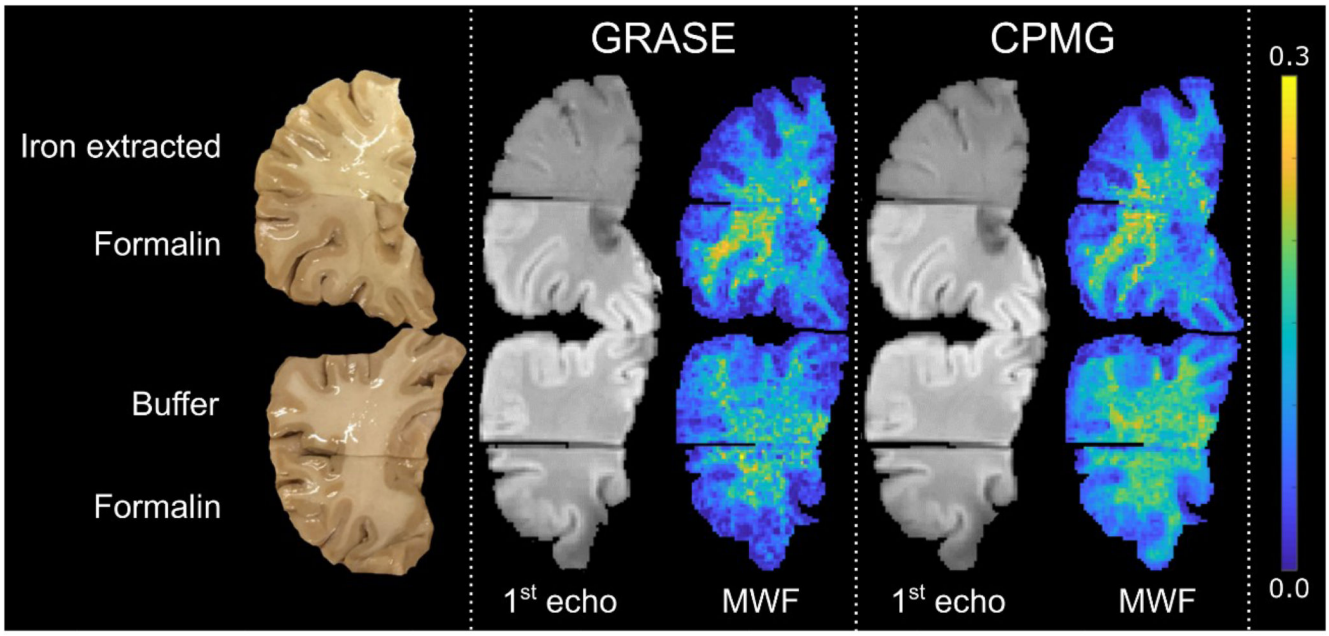

Fig. 3.

The top row shows a brain slice, the corresponding images of the 1st echo (TE = 10 ms) and MWF maps assessed using the GRASE and CPMG sequence, respectively. The brain slice was cut into two parts, where the upper part underwent 12 days of iron extraction and the lower part was kept in formalin as reference. A clear change in image contrast and decrease in MWF is observed in the iron extracted part compared to the reference part. The bottom row shows a second brain slice, out of the same brain, the corresponding images of the 1st echo (TE = 10 ms) and MWF maps for both the GRASE and CPMG sequence. The brain slice was cut into two parts where the upper part was kept in the buffer solution without iron chelator and the lower part in formalin for 12 days. No change in image contrast and MWF was observed in the buffer treated part compared to the part stored in formalin.

Europe PMC Funders Author Manuscripts

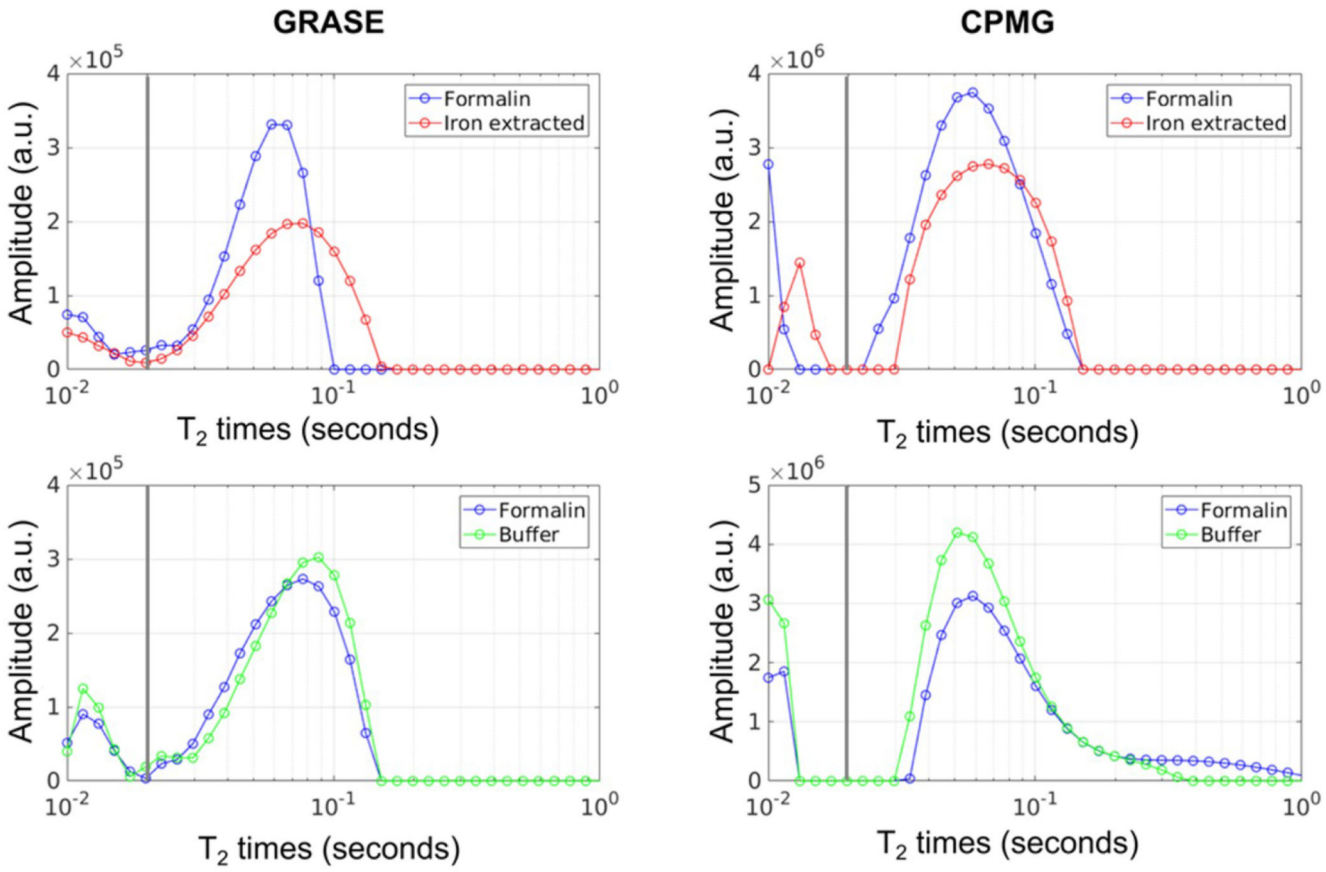

Fig. 4.

Representative white matter T_2 distributions of a brain slice stored in formalin compared to a brain slice where chemical iron extracted was performed (top row). The bottom row shows representative T_2 distributions of a brain slice stored in formalin compared to a brain slice treated with buffer solution. All brain slices used for this figure were from the same brain. The T_2 distributions were assessed using the GRASE and CPMG sequence. The vertical solid gray line represents the cut-off between the short and long T_2 components.

Europe PMC Funders Author Manuscripts

Europe PMC Funders Author Manuscripts

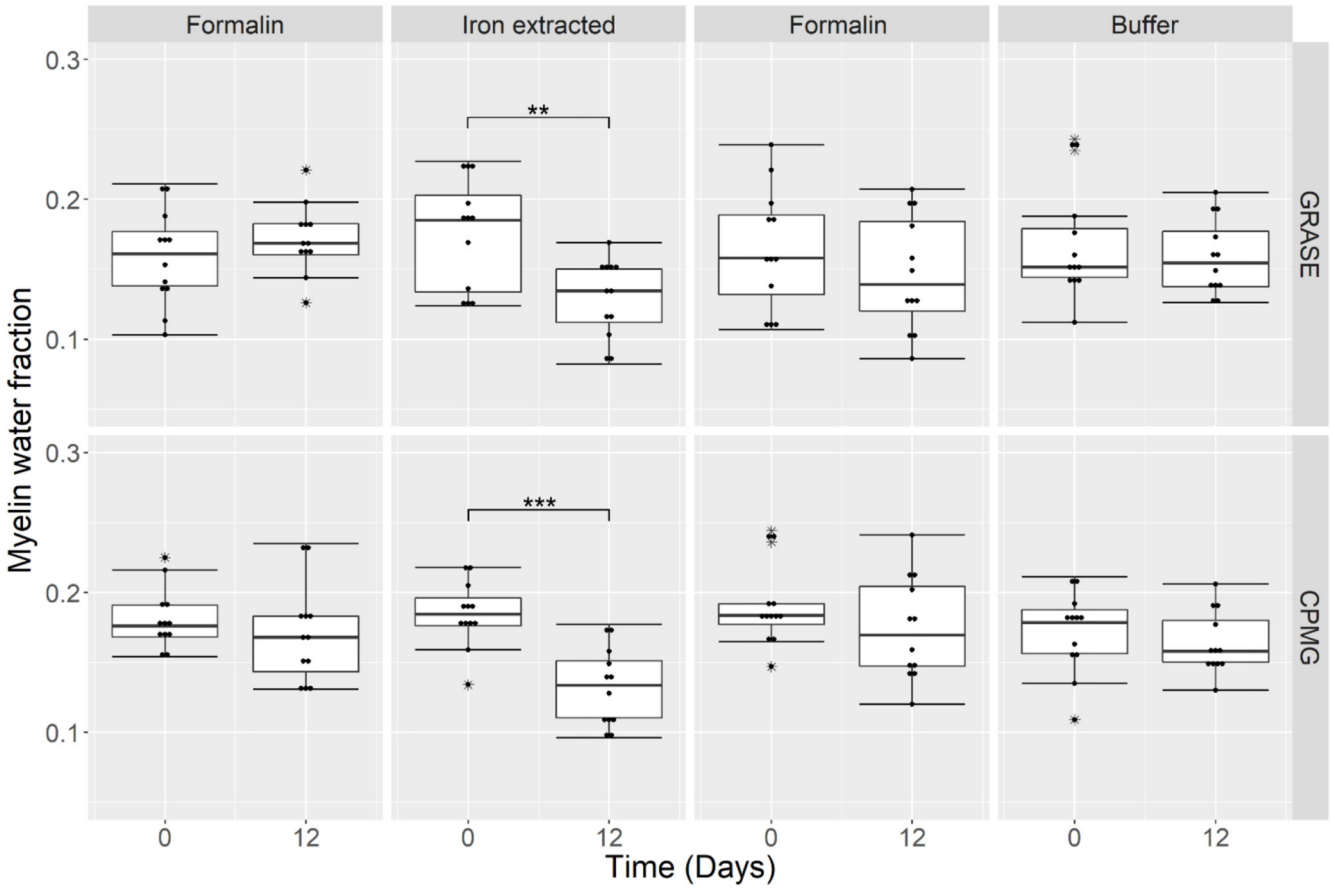

Fig. 5.

Myelin Water Fraction assessed in WM at Day 0 and Day 12 of four brain slices where one half of each slice was kept in formalin and the other half underwent iron extraction, and in four additional brain slices where one half or each slice was kept in formalin and the other half in the buffer solution, respectively. A significant decrease in MWF is observed after 12 days of iron extraction for both the GRASE ($p = 0.003$) and CPMG ($p < 0.001$) sequence. No significant change in MWF was observed after buffer storage and in the formalin brain slices.

Europe PMC Funders Author Manuscripts

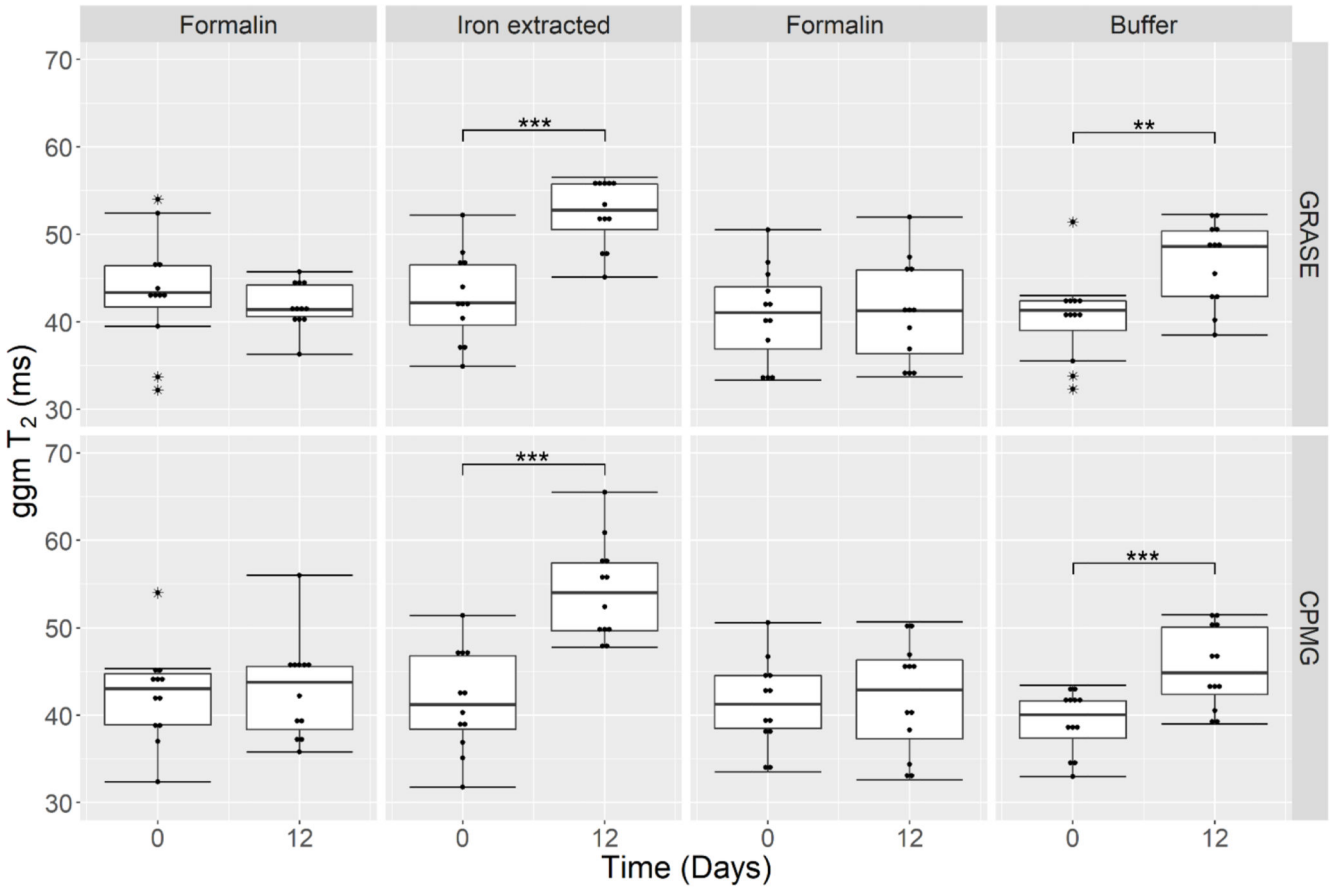

Fig. 6.

Global geometric mean (ggm) T_2 assessed in WM at Day 0 and Day 12 of four brain slices where one half of each slices was kept in formalin and the other half underwent iron extraction and in four additional brain slices where one half or each slice was kept in formalin and the other half in the buffer solution respectively. A significant increase in T_2 is observed after 12 days of iron extraction for both the GRASE ($p < 0.001$) and CPMG ($p < 0.001$) sequence and after 12 days of buffer storage for both the GRASE ($p = 0.003$) and CPMG ($p < 0.001$) sequence. T_2 of the formalin reference samples was stable for both the GRASE and CPMG sequence.

Europe PMC Funders Author Manuscripts

Neuroimage. Author manuscript; available in PMC 2021 May 17.

Table 1

Summarized median and range of the global geometric mean (ggm) T_2 relaxation time, myelin water fraction (MWF), short geometric mean (sgm) T_2 relaxation time, intra- and extracellular water fraction (mfr) and intra- and extracellular water geometric mean (mgm) T_2 relaxation time. Values were assessed in WM of four brain slices where one half of each slice was kept in formalin and the other half underwent iron extraction and four brain slices where one half of each slice was kept in the buffer solution without iron chelator and the other half in formalin. The relative change between day 0 and day 12 was calculated and the statistical difference was assessed.

		GRASE						CPMG					
		Day 0		Day 12				Day 0		Day 12			
		Median	Range	Media	Range	Change (%)	P-val	Median	Range	Median	Range	Chang e (%)	P-val
	ggm T_2 (ms)	43.4	(32.2-54.0)	41.4	(36.3-45.7)	-5	0.3	43.1	(32.4-54.0)	43.8	(35.8-56.0)	2	0.62
	MWF	0.16	(0.10-0.21)	0.17	(0.13-0.22)	6	0.23	0.18	(0.15-0.23)	0.17	(0.13-0.24)	-6	0.52
Formalin	**sgm T_2 (ms)**	12.4	(10.3-14.9)	11.7	(10.2-15.8)	-6	0.75	10.5	(10.0-11.7)	12.3	(10.0-17.6)	17	**0.03**
	mfr	0.83	(0.79-0.89)	0.82	(0.75-0.87)	-1	0.34	0.8	(0.72-0.84)	0.82	(0.76-0.87)	3	0.42
	mgm T_2 (ms)	55	(42.6-57.8)	53.1	(43.6-56.5)	-3	0.69	54.4	(44.7-57.5)	53.5	(43.7-57.1)	-2	0.35
	ggm T_2 (ms)	42.2	(34.9-52.2)	52.3	(45.1-56.5)	24	**< 0.001**	41.2	(31.8-51.4)	54	(47.8-65.5)	31	**< 0.001**
	MWF	0.19	(0.12-0.23)	0.14	(0.08-0.17)	-26	**0.003**	0.18	(0.13-0.22)	0.13	(0.10-0.18)	-28	**< 0.001**
Iron extracted	**sgm T_2 (ms)**	12.8	(11.6-14.1)	12.2	(11.1-12.9)	-5	**0.049**	10.1	(10.0-12.0)	13.1	(10.4-15.0)	30	**0.007**
	mfr	0.81	(0.77-0.88)	0.85	(0.80-0.92)	5	**0.003**	0.79	(0.71-0.82)	0.85	(0.73-0.90)	8	**0.005**
	mgm T_2 (ms)	55.3	(44.2-61.4)	64.1	(53.8-71.1)	16	**< 0.001**	54.1	(43.6-58.6)	65	(56.1-71.0)	20	**0.003**
	Ggm T_2 (ms)	41.1	(33.3-5-.5)	41.3	(33.7-52.0)	0	0.58	41.3	(33.5-50.6)	42.9	(32.6-50.7)	4	0.9
	MWF	0.16	(0.11-0.24)	0.14	(0.09-0.21)	-13	0.21	0.18	(0.15-0.25)	0.17	(0.12-0.24)	-6	0.12
Formalin	**sgm T_2 (ms)**	12.5	(10.0-16.60	11.3	(10.0-13.8)	-10	0.05	12.3	(10.2-15.6)	11.2	(10.0-13.6)	-9	0.06
	mfr	0.84	(0.76-0.89)	0.86	(0.79-0.96)	2	0.18	0.82	(0.76-0.85)	0.82	(0.76-0.88)	0	0.27
	mgm T_2 (ms)	52.7	(43.4-58.8)	50.8	(43.1-58.5)	-4	0.5	53.4	(44.4-67.2)	55.3	(43.3-66.7)	4	0.9
	ggm T_2 (ms)	41.3	(32.3-51.4)	48.6	(38.5-52.3)	18	**0.003**	40.1	(33.0-43.4)	44.9	(39.0-51.5)	12	**< 0.001**
	MWF	0.15	(0.11-0.24)	0.15	(0.13-0.21)	0	0.42	0.18	(0.11-0.21)	0.16	(0.13-0.21)	-11	0.17
Buffer	**sgm T_2 (ms)**	12.4	(10.0-17.0)	11.7	(10.0-14.6)	-6	0.35	10.4	(10.0-15.4)	11.1	(10.0-12.5)	7	0.78
	mfr	0.85	(0.76-0.88)	0.84	(0.80-0.87)	-1	0.72	0.82	(0.79-0.89)	0.84	(0.79-0.85)	2	0.26
	mgm T_2 (ms)	51.5	(38.8-59.7)	63.5	(46.7-72.0)	23	**< 0.001**	52.3	(40.9-57.3)	59.5	(50.7-73.6)	14	**< 0.001**